DNA rotational positioning in a regulatory nucleosome is determined by base sequence. An algorithm to model the preferred superhelix

Benjamín Piña[1,2+], Mathias Truss[1], Heiko Ohlenbusch[3], Johan Postma[2] and Miguel Beato[1*]
[1]Institut für Molekularbiologie und Tumorforschung, Emil-Mannkopff-Straße 2, D-3550 Marburg, [2]EMBL Computer Graphics, Meyerhofstrasse 1, Postfach 102209 D-6900 Heidelberg, FRG and [3]Université Louis Pasteur de Strasbourg, Faculté de Médicine, Institut de Physique Biologique, 4 rue Kirschleger, F-67085 Strasbourg Cedex, France

Received August 7, 1990; Revised and Accepted October 26, 1990

ABSTRACT

MMTV-LTR sequences −190/−45 position a histone octamer both *in vivo* and *in vitro*. Experimental evidence suggested that nucleosome rotational positioning is determined by the DNA sequence itself. We developed an algorithm that is able to predict the most favorable path of a given DNA sequence over a histone octamer, based on rotational preferences of different dinucleotides. Our analysis shows that these preferences are sufficient for explaining the observed rotational positioning of the MMTV-LTR nucleosome, at one base pair accuracy level. Computer-generated 3-D models of the experimentally calculated and predicted MMTV-LTR nucleosome show that the predicted orientation is fully compatible with the currently available data in terms of accessibility of relevant sequences to regulatory proteins.

INTRODUCTION

Several lines of evidence suggest an important role of chromatin organization in the control of gene expression. Transcriptional induction of several genes is accompanied by major chromatin structural changes leading to the creation of hypersensitive DNaseI cutting sites (1,2). Strictly regulated genes have a precise nucleosome positioning over their regulatory regions; this structured chromatin undergoes specific changes upon transcriptional induction (3−6). Recent results demonstrate that nucleosome positioning directly effects the function of *cis*-acting DNA elements *in vivo* (7).

The long terminal repeat of the mouse mammary tumor virus (MMTV-LTR), a classical model for hormone regulated promoter/enhancer systems (8), is emerging as an excellent model for structural studies on chromatin. Up to six nucleosomes are precisely phased over MMTV-LTR sequences from −1019 to +136 (5). This phasing can be reproduced in chromatin reconstitution experiments (9,10,11). The promoter proximal region of MMTV-LTR contains a set of binding sites for hormone receptors as well as a binding site for nuclear factor I (NFI). This region has been shown to be essential for hormonal induction through the MMTV-LTR (12−14). One striking feature of the nucleosome positioning over this region is that all the relevant motifs are covered by a single histone octamer, forming the so-called nucleosome B (5). Hormone administration results in the dissociation or destabilization of this nucleosome B (2,5). Nucleosome disruption appears to be required for binding of NFI, as this factor fails to bind MMTV chromatin in non-induced states either *in vivo* and *in vitro* (10,15). Precise orientation of the MMTV-LTR DNA double helix over the histone octamer modulates the access of transcription factors to their binding sites, allowing binding of progesterone and glucocorticoid receptors but excluding NFI. This suggests a highly specific role of nucleosome positioning on transcriptional control through the MMTV-LTR (10).

The factors responsible for specific orientation of the DNA double helix around the histone octamer (so-called rotational positioning, 16) are not completely understood. Small circular DNA molecules containing the appropriate MMTV-LTR sequences tend to adopt the same conformation as that in nucleosome B (11), showing that this particular conformation is not histone-dependent. Here we present an algorithm, based on the rotational preferences of dinucleotides in nucleosomes,that is able to predict the rotational positioning of DNA wrapped arround the histone octamer. 3D models are used to compare the experimental determined conformation of the MMTV-LTR sequences in nucleosome B with the predicted one. This comparison indicates that the rotational preference of dinucleotides is sufficient to explain the rotational positioning observed in MMTV nucleosome B.

* To whom correspondence should be addressed

+ Present address: Massachusetts Institute of Technology, 77 Massachusetts Ave, Cambridge, MA 02139, USA

DATA, ALGORITHM AND PROGRAMS

Positioning of the MMTV-LTR DNA sequences

We have previously mapped the path of MMTV-LTR DNA sequences −190/−45 around the histone octamer using *in vitro* reconstituted MMTV nucleosome B and analyzing it with both DNaseI digestion and the hydroxyl radical (HR) footprinting technique (10). Although using these techniques it is possible to determine the orientation of all base pairs on the sequence, we have focused on base pairs having their minor grooves facing exactly outwards from the histone octamer. The position of these base pairs can be easily calculated as average of consecutive HR maxima and DNaseI cutting sites on the lower and upper strands (Table I). Following the criteria from Drew and Calladine (17), we define the orientation of these base pairs as a 0-degree phase angle; a phase angle of 180 degrees corresponds therefore to base pairs having their minor grooves facing inwards. In all calculations, base pair positions are given relative to the MMTV CAP site.

Algorithm

Our algorithm uses the rotational preference matrix for dinucleotides and its associated rotational fit calculation procedure, which are set out in Drew and Calladine (17); the matrix was derived statistically from 177 aligned chicken core sequences. The program calculates the total angular preference for any given DNA sequence in 24 possible rotational orientations It calculates the orientation of every dinucleotide contained in a given sequence, once an initial phase orientation, a_0 has been introduced. The orientation of dinucleotide n_i,n_{i+1} is calculated as

$$a_i = a_0 + 360*(i-1)/p$$

where p is the pitch of the DNA molecule. From this orientation value, rotational preferences (17) for every dinucleotide on the sequence are calculated, and their product (π_{a0}) is used as a measurement of the total preference of the entire sequence for this particular orientation. Successive 15-degree rotation of the DNA helix by increasing the value of a_0, and calculation of the corresponding π values gives the total orientation preference for the whole molecule in the 24 possible different orientations. Finally, the program chooses as best that a_0 giving the highest π value. The exact orientation of all nucleotides on the DNA helix is determined by a_0 and p. Different orientations of the DNA molecule are characterized by positions of base pairs on each DNA turn with the closest to 0/360-degree phase angles—i.e. with the most exposed minor grooves.

3-D representation of an oriented DNA superhelix

We have used the program SUPERHELIX in order to produce a 3-D model of the DNA superhelix corresponding to MMTV-LTR sequences at the calculated orientation for the highest π value. This program is a routine option of the macromolecular graphics system available at the EMBL Molecular Graphics Group. It calculates XYZ coordinates of a B DNA superhelix of any given sequence; the characteristics of the DNA superhelix are determined by the following input data:

1—DNA sequence

2—Pitch of the DNA molecule. This parameter is introduced as torsional advance per nucleotide (360/p) and calculated from the input DNA pitch.

3—Radius of curvature of the DNA. The default is chosen to give an external radius of 11 nm (18).

4—Pitch of the DNA superhelix. The default is −27.5 nm, as corresponding to a left-handed nucleosomal DNA superhelix (18).

5—Orientation of the first base pair. This value determines the orientation of the whole DNA molecule relative to the curvature radius. It is calculated from the prediction program (for predicted orientations) or adjusted in order to give the observed orientation.

These XYZ coordinates can routinely be interpreted by the EMBLFRODO[x] program (19) and displayed on an Evans and Southerland MPS monitor. They are compatible with different molecular graphic programs after transformation into Brookhaven-type of data file.

RESULTS

Calculation of the preferred DNA pitch

Our algorithm strongly depends on the DNA pitch for calculating the orientation of the dinucleotides contained in a given sequence. DNaseI digestion of MMTV-LTR sequences −190/−45 wrapped around the histone octamer gives an average pitch of 10.20 bp per DNA turn (10). We have calculated the preferential orientation of these MMTV-LTR sequences using input DNA pitches ranging from 10.00 to 10.40 bp/turn. The results are shown in figure 1. The optimal π value, i.e., the total preference of the complete sequence for the best orientation at a given pitch,

Upper strand		Average	Lower strand	
HR	DNaseI		DNaseI	HR
	-53	-54	-55	
-62	-63	-64.5	-65	-68
-72	-73	-74	-75	-76
-82	-83	-84.25	-85	-87
-92	-93	-94.25	-95	-97
-102	-103	-104.25	-105	-107
-112	-113	-114.5	-116	-117
-122	-122	-124.5	-126	-128
-133	-133	-135.75	-138	-139
-144	-146	-147	-149	-149
-154	-155	-156.75	-158	-160
-166	-165	-167.5	-167	-172
-177	-177	-178.25	-178	-181
	-185	-187	-189	

Table I. Orientation of the MMTV-LTR DNA double helix over the histone octamer. The data show DNaseI cutting sites (DNaseI) and Hydroxyl radical maxima (HR) over the MMTV-LTR sequences −190/−45, for the upper and the lower strand. The column labelled 'Average' displays the average between the four data from both strands. These values are the best possible estimation of the position of base pairs with the minor groove pointing exactly outwards the histone octamer. Positions are given relative to the MMTV-LTR CAP site.

peaks at a DNA pitch value of 10.10 bp/turn (Figure 1, solid bars). This value is clearly lower than the experimentally calculated pitch. We consider this value as the theoretically preferred DNA pitch for these MMTV-LTR sequences.

Figure 2 shows the π values for the 24 different a_0 using an input pitch of 10.10. A very prominent peak is observed, indicating that the analyzed sequence has a strong preference for one particular orientation over the others. Corresponding calculations with different input DNA-pitches give similar plots; however, pitches corresponding to a low optimal π values have also a less prominent peak, indicating that alternative orientations are possible (not shown). For further calculations, only orientations giving the highest π values for each input pitch will be considered.

Comparison between predicted and observed MMTV nucleosome

In order to compare the predicted path of the MMTV-LTR DNA over the histone octamer with the experimental data we compared the 0-degree positions predicted by the algorithm with the averaged values displayed on table I. We have used two parameters, in order to establish the fitting of the predicted orientation to the experimental one. The first parameter is the difference between observed and predicted 0-degree positions ($P_{obs.}-P_{cal.}$). It gives us an indication about both the magnitude and the sense of the deviation of the predicted values relative to the experimental ones (Fig. 3). Summation of all these differences for the complete sequence gives an estimation of the fit of the calculated total orientation to the experimental data. A total deviation of 0 would mean that theoretical and experimental orientations of the DNA molecule are identical. Figure 1 shows the values of $\Sigma(P_{obs.}-P_{cal.})$ for different input DNA pitches from 10.00 to 10.40 base pairs (bp)/turn (hatched bars). These values fluctuate from +10 for a pitch of 10.25 to −7 for a pitch of 10.00. The theoretically preferred DNA pitch of 10.10 bp/turn gives a value of −2.0. This value indicates that the predicted 0-degree positions are, on avarage, 0.14 bp apart from the observed ones. The average deviation between observed and predicted values for the worst case (DNA pitch = 10.25 bp/turn) is about 0.71 bp.

Two conclusions can be drawn from these calculations. First, the theoretically predicted orientations show very little dependance on the input DNA pitch. The highest average difference between two of them is about 1.2 bp, the observed values lying approximately on the center of this range. Second, all these orientations (irrespective to the input DNA pitch) are very close to the experimental data. Most of them show average deviations smaller than 0.3 bp.

Analysis of $P_{obs.}-P_{cal.}$ values for different pitches at the different positions of the sequence show that these values follow an approximately sinusoidal pattern (Figure 3). This pattern is more clearly seen if values from a single DNA pitch are analyzed (Figure 3, DNA pitch = 10.10 bp/turn). Our interpretation is that this sinuosity pattern is due to differences between the calculated and the experimental pitch that are not adequately reflected by the first parameter. In order to quantify these deviations, we have introduced a second parameter, $\Sigma(P_{obs.}-P_{cal.})^2$. Its value for the different input pitches is shown in figure 1 (shadowed bars). A

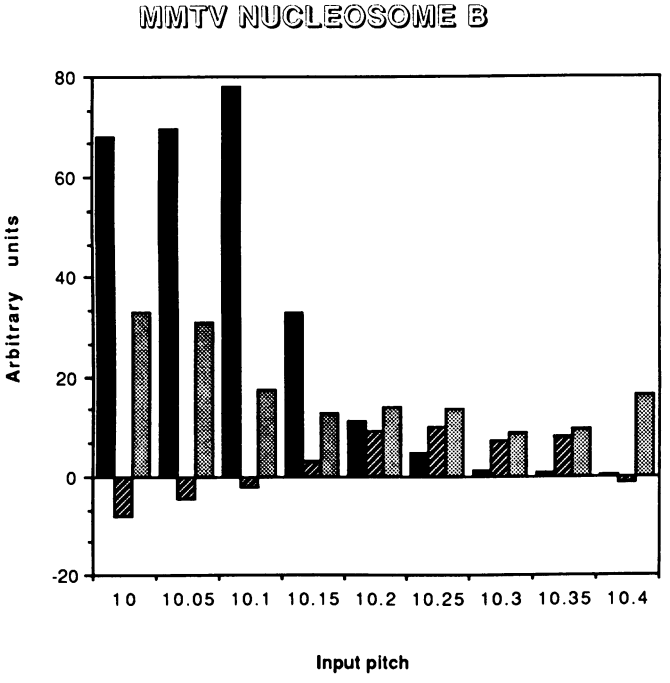

Figure 1. Effect of the DNA pitch on the predicted orientation. MMTV-LTR sequences −190/−45 were analyzed using different input pitches from 10.00 to 10.40. Solid bars indicate the π value of the best orientation at the different pitches. Note the maximum at pitch 10.10. Hatched bars represent the summation of the differences between the observed positions having the minor groove facing exactly out and their calculated counterparts, $\Sigma(P_{obs.}-P_{cal.})$. These values give an indication of the deviation of the calculated orientation of the molecule relative to the observed one. Shadowed bars indicate the summation of the square of the previous differences, $\Sigma(P_{obs.}-P_{cal.})^2$.

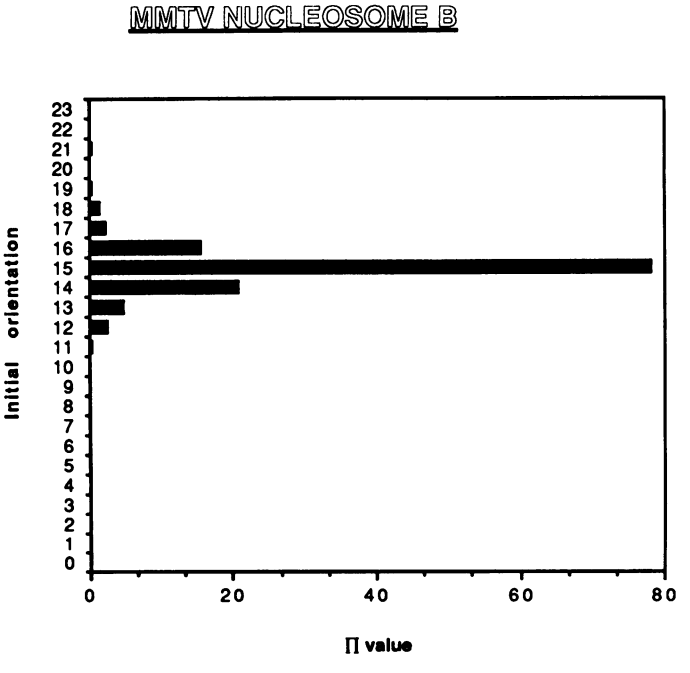

Figure 2. Measurement of the preference of MMTV-LTR sequences for a given orientation. π values from the 24 calculated orientations for the MMTV-LTR sequences are shown. The theoretically preferred value of the DNA pitch = 10.10 bp/turn has been used for these calculations.

value of 0 would mean that predicted and observed 0-degree positions are identical for every DNA turn along the complete sequence; positive and negative deviations would not compensate one each other. These values show also a small dependance on the input DNA pitch. The maximum (i.e., the worse adjust) is obtained at an input pitch of 10.00 bp/turn (33.13) and the minimum (the best one) at a pitch of 10.30 bp/turn (8.62). The square root of the average of these values gives an estimation of the standard deviation of the calculated 0-degree positions from the observed ones. The corresponding values are ±1.54 bp for the worse adjustment and ±0.78 bp for the best one. The value corresponding to the theoretically preferred pitch of 10.10 bp/turn is ±1.13 bp.

Computer modelling of the predicted MMTV-LTR superhelix

We have used the computer graphics facilities at EMBL for visualizing the fit of the calculated MMTV-LTR superhelix relative to the experimental data. Figure 4A and B shows four stereo pairs corresponding to predicted and observed MMTV-LTR superhelices respectively. The theoretically optimal DNA pitch of 10.10 bp/turn was used for the predicted superhelix; the experimentally determined one of 10.20 bp/turn was chosen for the observed superhelix. For better visualization, the approximately 1.8 superhelical turns of the 146 bp around the histone octamer have been divided in two halves, one containing MMTV-LTR sequences −190/−121 and the second sequences −120/−45. The four TGTTCT motifs for progesterone and glucocorticoid receptors at −175 (BSI), −119 (BSII), −98 (BSIII) and −83 (BSIV), as well as the distal part of the imperfect palindrome at −184/−179 (BSI), are labelled by filling their desoxyribose rings black and by using a slightly broader line drawing. The two TGGA motifs of the palindromic NFI binding site at −75/−72 and −66/−63 are labelled in the same way. The position of these motifs on the MMTV-LTR sequences are shown in a schematic representation on figure 4C.

Inspection of these 3-D models shows the similarity between the predicted and the observed superhelix. Relevant sequences display in both of them a very similar orientation relative to the curvature radius (i.e., the histone octamer in the nucleosome). These predicted orientations have to be considered in terms of accessibility of regulatory proteins to their cognate sequences on the MMTV nucleosome. Hormone receptors, as well as NFI, recognize specific DNA sequences through the DNA major groove (21,22). Therefore, if we consider a nucleosome, only DNA sequences presenting the major groove facing out are accessible to binding (10). In our 3-D model, the major grooves of BSI and IV are accessible whereas those of BSII and III are clearly hidden in the predicted MMTV nucleosome confirming the experimental data (10). The NFI binding site seems to be slightly more exposed in the predicted MMTV nucleosome than is reflected in the published data (10); however, the angular difference between the observed and the calculated orientation of these binding sites (about 1 bp) falls within the intrinsic precision of our calculations. This means that accessibility of the different binding sites in the reconstituted MMTV-LTR nucleosome (10) is closely predicted by the algorithm.

DISCUSSION

Detailed analysis of chromatin structure demonstrates that nucleosome positioning has two different implications. The first and best known is that nucleosomes are specifically placed over certain regions of the DNA sequence, in a way that determines which base pairs are covered by the histone octamer and which ones lie on the linker DNA. This is called 'translational positioning' (16,17). The second aspect is related to the path of the nucleosomal DNA over the histone octamer, the so-called

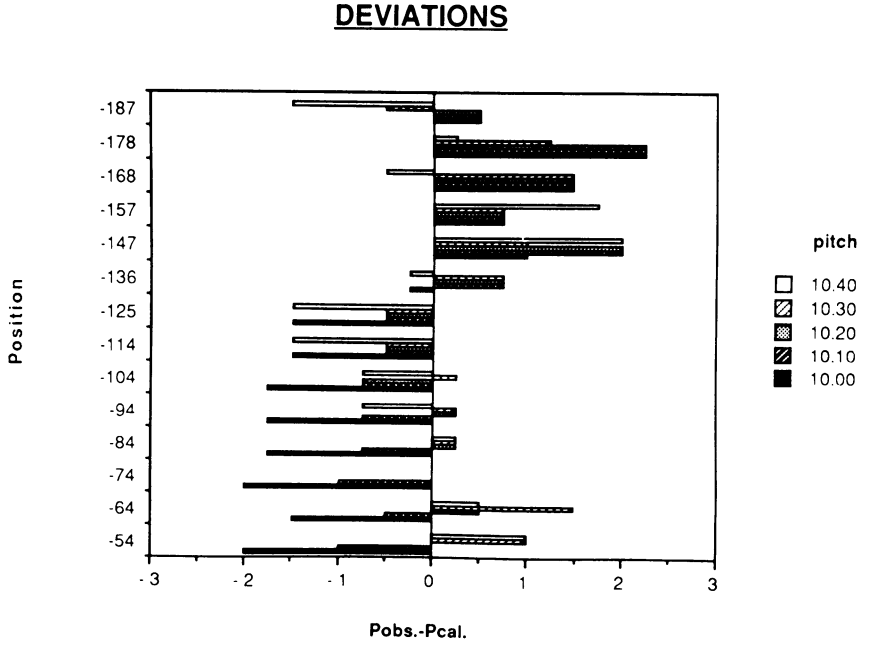

Figure 3. Deviation of the calculated data from the experimental values. Positions with their minor groove pointing out were used for estimating the fitting of the calculated orientation for the different parts of the MMTV sequence. This calculation uses the theoretically preferred DNA pitch (10.10 bp/turn, fig. 1) and the preferred orientation (Fig. 2).

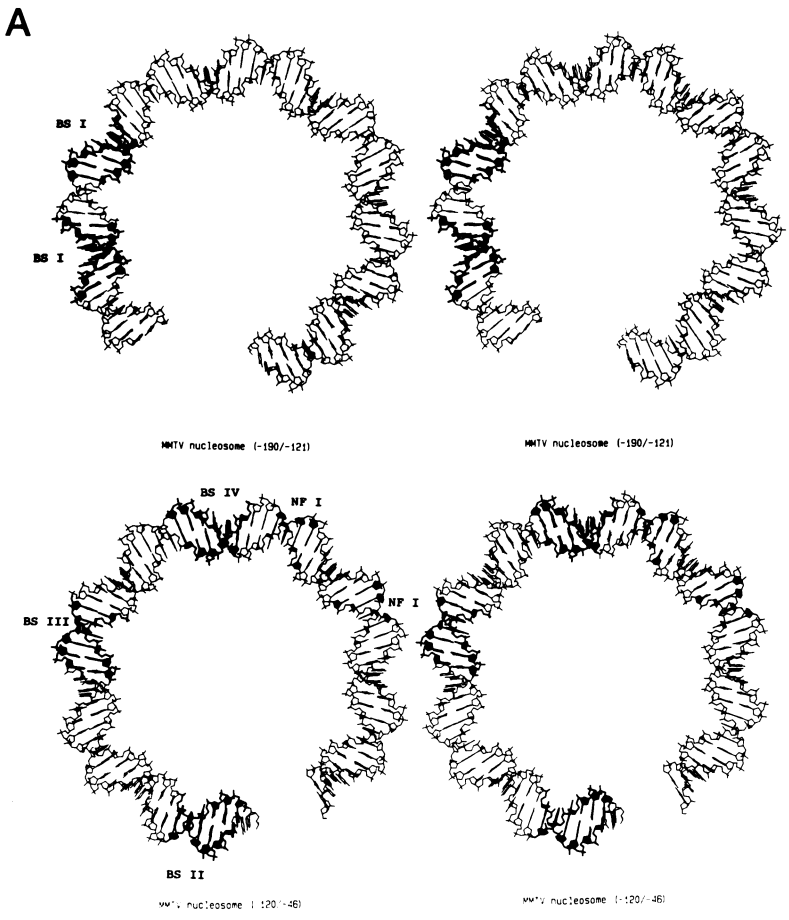
A
BS I
BS I
MMTV nucleosome (-190/-121)
MMTV nucleosome (-190/-121)
BS IV
NF I
NF I
BS III
BS II
B
Predicted MMTV nucleosome (-190/-121)
Predicted MMTV nucleosome (-190/-121)
Predicted MMTV nucleosome (-120/-46)
Predicted MMTV nucleosome (-120/-46)

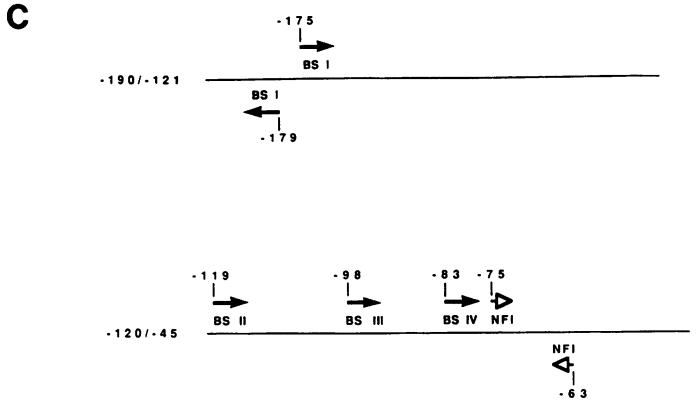

Figure 4. A) and B). Stereo pairs of the MMTV-LTR sequences −190/−45 wrapped around the nucleosome. For easy visualization, the 1.8 turns of the DNA around the histone octamer have been divided in two halves, −190/−121 and −120/−45. Observed (B) and predicted (A) orientations are shown. The B model was drawn using the observed DNA pitch for the MMTV-LTR nucleosome B (10.20 bp/turn, ref. 10) and the orientation of the whole molecule was set in order to maximize the exposure of the minor grooves of the base pairs listed in Table I. For the A model, the theoretically preferred DNA pitch was used (10.10 bp/turn, fig. 1) and the orientation of the DNA molecule was set by a computer program using the algorithm described in the text. Binding sites for the GR and PR are labelled BSI, BSII, BSIII and BSIV. NFI binding site is also labelled. C) Schematic representation of the positions of relevant motifs over MMTV-LTR sequences −190/−121 (top) and −120/−45 (bottom). Figures represent the position of the first 5′ bp of the given motif and are referred to the MMTV-LTR CAP site. Binding sites for GR, PR (black arrows) and NFI (open arrows heads) are indicated.

	DNA pitch		Average deviation	Standard deviation
	Observed	Predicted	$\Sigma[P_{obs.} - P_{pre.}]/n$	$\sqrt{\Sigma[P_{obs.} - P_{pre.}]^2/n}$
MMTV nucleosome B	10.20	10.10	-0.14	1.13
MMTV nucleosome A	10.05	10.00	+0.35	0.71
Xenopus 5s nucleosome	10.40	10.35	-0.25	0.74

Table II. Analysis of DNA sequences from MMTV-LTR nucleosomes B (−190/−45) (9, this work), A (+30/+175) (11) and from the *Xenopus* 5S gene (20). The table shows the observed and predicted DNA pitch, the average deviation between the observed and predicted 0-degree positions and the corresponding standard deviations. The corresponding formula are shown over the corresponding column. DNA pitches are given in bp/turn; deviations in bp. The 'observed' repeat for the *Xenopus* 5S gene corresponds to our estimation of the 0-degree positions from the published data (see the text).

'rotational positioning' (16,17). This means that on the nucleosomal DNA some base pairs tend to be oriented with their minor grooves in contact with the histone octamer (and therefore, their major grooves face outwards) whereas others prefer to orient their minor grooves in the opposite way. Given a defined position of the double helix the different accessibility of the minor groove results in defined patterns of DNaseI digestion (10,16,17) and hydroxyl radical attack (10). Moreover, the differential access of regulatory proteins to their cognate sequences when wrapped around the histone octamer, depending on the orientation of the major grooves of these sequences (10), can explain the *in vivo* observed binding pattern of these proteins (15). This pattern can not be fully explained in terms of the affinity of the proteins for free DNA (10).

Statistical analysis of chicken erythrocyte core sequences demonstrate that the different base pairs are not evenly distributed along nucleosomal DNA. Runs of A,T are predominantly found in DNA sequences exposing their major grooves, whereas runs of G,C tend to orient their minor grooves facing out (16,17,20,23). Theoretical and crystallographic analysis correlate this uneven distribution of base pairs with sterical hindrances between consecutive bases in bent DNA. These effects result on each combination of adjacent base pairs (e.g., AC, TT, GC etc.) having a preferred roll angle—i.e., a preferred orientation relative to the bending radius (24). On this orientation, the energy required for bending is minimal. If DNA is forced to form a superhelix around the histone octamer or a circle in a small close DNA molecule, it will tend to minimize its energy by adopting a configuration where the orientation of the different base pairs is as close as possible to the optimal one, considering the given constrains (DNA pitch, curvature radius, etc.). This will ultimately result in a specific orientation of the DNA molecule relative to the center of curvature, i.e., in a defined rotational positioning.

Previous work demonstrated that MMTV-LTR sequences −190/−45 are wrapped around the histone octamer showing a clear rotational positioning (10). This positioning appears to be sequence-related, as small circular DNA molecules made on the same sequences adopt a very similar configuration even in the absence of histones (11). We have submitted these DNA sequences to an algorithm that is a direct application of the rotational preference matrix of different dinucleotides from aligned DNA sequences of chicken erythrocyte core particles, as published by Drew and Calladine (17). Our analysis demonstrate that this algorithm is able to predict the observed orientation with a high accuracy, with an average deviation of

only 0.14 ± 1.13 bp. Clearly, the rules applying for the chicken erythrocyte core sequences also apply for the MMTV-LTR DNA.

It must be pointed out that no data from our sequences, or from related ones, are included in the algorithm itself. No *ad hoc* assumptions have to be made in order to adjust the theoretically preferred orientation to the experimental data. The only input from our experimental data is the sequence itself and the limits of the nucleosome, as determined by ExoIII digestion (10). In order to make sure that possible small errors on the determination of the nucleosome limits would not influence the final prediction, we have subjected the MMTV-LTR region −220/−10 to the same sequence analysis; no significant differences on the predicted orientation were found (not shown).

Our analysis is somewhat similar to the algorithm of Calladine and Drew (ref. 24). This algorithm uses crystallographic data in order to calculate the preferred roll angles for the different dinucleotides. Further refinements with statistical considerations from Ref.23 produces a model able to adequately locate the dyad axis of an *in vitro* reconstituted nucleosome from *Xenopus* 5S RNA gene (24,25). Calcualtion of the rotational fit of the DNA molecule by addition of hte likelihoods of the different dinucleotides has also been shown to be able to predict the positioning of at least some nucleosomes over Xenopus 5S gene, although some structural considerations are required (17). In the present work, we have used exclusively statistical data from Ref.17, without any further consideration on the nucleosome structure or any nucleosome model, to predict the orientation of relevant regulatory sequences. We think that the possibility of producing a matrix of 3-D coordinates of the DNA molecule on the predicted orientation featured by our program is possibly the best approach.

In order to assess the general validity of the algorithm, we have subjected data from other well characterized nucleosomes to a similar analysis. We have analyzed data from nucleosome cores reconstituted on two different DNA sequences: the *Xenopus* 5S RNA gene (ref. 25) and the MMTV-LTR nucleosome A (11). For the first one, we have had to estimate the 0-degree positions from the published data, that gives a detailed plot of relative probabilities of DNaseI cutting in both strands (25). Accepting the possible error we may have introduced in our estimation, the results (Table II) show that our algorithm predicts with high accuracy the observed orientation for both sequences. Thus, it seems to be able to successfully orient DNA sequences from very different origins.

One intriguing aspect of our analysis of the MMTV-LTR sequences is the apparent disagreement between the DNA pitch theoretically required for optimal bending (10.10 bp/turn) and the experimentally obtained one (10.20 bp/turn). To some extend, this discrepancy is also found in the other two analyzed sequences (Table II). This difference implies that the first and last observed 0-degree positions (−54 and −187, table I) are, on average, 1.25 bp further from the nucleosome center than it would be expected from the theoretically preferred positioning. One simple possibility is that some DNA sequence feature(s) not considered by our algorithm may also contribute to the final positioning, and, therefore, our model requires further refinement. A second possibility concerns the way nucleosomal DNA is exposed to foreign agents. DNA bending on the nucleosome has been assumed to follow a cylindrical path (18,26). However, it is conceivable that the most probable directions of chemical or enzymatic attack may follow a different pattern, for example a spherical one. This would dissociate preferred bending from the observed data by approximately the same angular difference we observe. Further data will decide between these two possibilities, as well as how generally they can be applied.

Computer-generated 3-D models of predicted and observed MMTV nucleosome show that major groove accessibility of relevant motifs can be predicted by our algorithm. Angular differences between theoretical and experimental models are found near the ends of the sequence, namely on the distal region of BSI and on NFI binding sites. They can be explained by the differential pitch, as nucleosome centers are almost perfectly aligned. Even considering these differences as truly significant, the predicted accessibility of the relevant motifs would be only slightly modified. Therefore, the relative position of different dinucleotides on the DNA sequence seems to be sufficient by itself to explain most of the structural and functional properties of the MMTV regulatory nucleosome.

ACKNOWLEDGEMENTS

B.P. was supported by an EMBO Short Term Fellowship. The experimental work was supported by grants from the *Deutsche Forschungsgemeinschaft* and the *Fonds der Chemischen Industrie*.

REFERENCES

1. Eissenberg, J.C., Cartwright, I.L., Thomas, G.H. and Elgin, S.R.C. (1985) *Ann. Rev. Genet.* **19**, 485−536.
2. Zaret, K.S. and Yamamoto, K.R. (1984) *Cell* **38**, 29−38.
3. Benezra, R., Cantor, C.R. and Axel, R. (1986) *Cell* **44**, 697−704.
4. Almer, A., Rudolph, H., Hinnen, A. and Hörz, W. (1986) *EMBO J.* **5**, 2689−2696.
5. Richard-Foy, H. and Hager, G.L. (1987) *EMBO J.* **5**, 2321−2328.
6. Thomas, G.H. and Elgin, S.C.R. (1988) *EMBO J.* **7**, 2191−2201.
7. Simpson, R.T. (1990) *Nature* **343**, 387−389.
8. Beato, M. (1989) *Cell* **56**, 335−344.
9. Perlmann, T. and Wrange, Ö. (1988) *EMBO J.* **7**, 3073−3079.
10. Piña, B., Brüggemeier, U. and Beato, M. (1990) *Cell* **60**, 719−731.
11. Piña, B., Barettino, D., Truss, M. and Miguel Beato (1990) *J. Mol. Biol.* **216**, in press.
12. Scheidereit, C., Geisse, S., Westphal, H.M. and Beato, M. (1983) *Nature* **304**, 749−752.
13. Chalepakis, G., Arnemann, J., Slater, E., Brüller, H.J., Gross, B. and Beato, M. (1988) *Cell* **53**, 371−382.
14. Miksicek, R., Borgmeyer, U. and Nowock, J. (1987) *EMBO J.* **6**, 1355−1360.
15. Cordingley , M.G., Riegel, A.T. and Hager, G. (1987). *Cell* **48**, 261−270.
16. Travers, A.A. and Klug, A. (1987) *Phil. Trans. R. Soc. Lond.* 317, 537−561.
17. Drew, H.R. and Calladine, C.R. (1987) *J. Mol. Biol.* **195**, 143−173.
18. Finch., J.T., Lutter, L.C., Rhodes, D., Brown, R.S., Rushton, B., Lewitt, M. and Klug, A. (1977) *Nature* **269**, 29−36.
19. Carlson, C.N. and Bosshard, H.E. (1984) *J. Molec. Graphics* 2, 54−55.
20. Drew, H.R. and Travers, A.A. (1985) *J. Mol. Biol.* **186**, 773−790.
21. Scheidereit, C. and Beato, M. (1984) *Proc. Natl. Acad. Sci. USA* 81, 3029−3033.
22. de Vries, E., van Driel, W., van der Heuvel, S.J.L. and van der Vlied, P.C. (1987) *EMBO J.* **6**, 161−168.
23. Satchell, S.C., Drew, H.R. and Travers, A.A. (1986) *J. Mol. Biol.* **191**, 659−675.
24. Calladine, C.R. and Drew, H.R. (1986) *J. Mol. Biol.* **192**, 907−917.
25. Rhodes, D. (1985) *EMBO J.* **4**, 3473−3482.
26. Richmond, T.J., Finch, J.T., Rushton B., Rhodes, D. and Klug, A. (1984) *Nature* **311**, 532−531.